환경영향평가 제21권 제4호(2012) pp.553~565

연구논문

The Prediction Of Low Salinity Water Behavior Caused By Tidal Gate Extension In Yeongsan-River Estuary

Chul-Hui Kwoun* · Min-Sun Kwon* · Hun Kang* · Gyu-Sang Jang · Jeong-Bin Seo** · Kwang-Woo Cho*** · Jun-ho Maeng*****

Land Ocean Environment Co.,Ltd., Suwon, 443-470, Korea*, Rural Research Institute, Ansan, 426-908, Korea**
Korea Environment Institute, Seoul, 290, Korea***

(Manuscript received 21 February 2011; accepted 8 June 2011)

영산강 하구둑 배수갑문 확장 후 시간 변화에 따른 저염수 거동 예측

권철휘* · 권민선* · 강훈* · 장규상 · 서정빈** · 조광우*** · 맹준호*****

(주)국토해양환경기술단*, 한국농어촌공사 농어촌연구원**, 한국환경정책평가연구원***

(2011년 2월 21일 접수, 2011년 6월 8일 승인)

Abstract

영산강 하구에서 담수유입에 따른 저염수의 거동을 파악하기 위하여 EFDC 모델을 수행하였다. 모델의 수행은 홍수기 배수갑문 확장 전 · 후로 나누어 수행하였으며, 모델의 마지막 담수유입시점으로부터 16일 후 해역이 준 정상상태에 도달하기까지 저염수의 확산양상을 시간 경과순으로 살펴보았다. 그 결과, 담수유입이 멈춘 후에 저염수는 방류시점으로부터 약 6시간 경과 후에 배수갑문 전면 해역으로부터 해측으로 최대의 확산을 보였으며, 약 2~7일 후 염분의 분포 양상은 담수가 유입되기 전으로 회복되는 경향을 보였다. 한편, 배수갑문을 확장하기 전보다 배수갑문을 확장한 후에 담수유입 후 해역이 준 정상상태에 도달하는 시간이 더욱 짧았는데, 이는 시간당 방류량의 증가가 난류혼합을 강하게 하고, 해측으로 더 멀리 확산된 저염수는 외해수에 의해 보다 쉽게 혼합되기 때문인 것으로 판단된다. 따라서, 본 해역에서 일정한 양의 담수가 유입되는 경우, 저염수의 확산은 시간당 방류량이 크고 방류지속시간이 짧을수록 해역이 준정상상태에 도달하는 시간이 더욱 짧아질 것으로 사료된다.

주요어 : Yeong-san River, Low Salinity Water, Tidal Gate, Fresh Water Inflow

Corresponding Author : Min-Sun Kwon, Land Ocean Environment co., Ltd. Digital Empire Bldg., Yeongtong 2-dong, Yeongtong-gu, Suwon-si, Gyeong gi-do, Korea Tel: 80-31-695-3400 Fax: 80-695-3409 E-mail: hereforyou@empal.com

I. Introduction

The Yeongsan River Estuary Bank was built in 1981 to secure water for agricultural use and to prevent floods. Its tidal gate is currently being expanded as a response to an increase in floods caused by climate change and the resulting damages from the floods. Although at normal times there is no inflow of freshwater into the Yeongsan River Estuary, the expansion of the tidal gate is expected to cause a huge volume of freshwater to flow into the area, generating substantial impacts on the marine environment. Therefore, in order to minimize the damages to the marine environment, measuring the behavior of low salinity water caused by the expansion of the tidal gate should be prioritized. Much of the wetland found in the area near the Yeongsan River Estuary has been turned into reclaimed land, due to the constructions of the Yeongsan River Estuary Bank in February 1981, the Yeongam Seawall in April 1991, and the Geumho Seawall in March 1994 (Kang, 1996; Kang & Im, 1998). Such artificial environmental change brought much change in the physical characteristics, water quality, and ecology of Yeongsan-river estuary. Annual average high tide level and yearly highest high water level of Mokpo harbor decreased individually about 7cam and 15cam due to construction of Yeongsan-river estuary and Yeongam seawall. Also, after 1991, the construction of Yeongam-Geumho seawall, annual average high tide level increased 14.9cm additionally(Lee and Shin, 1999). Such change of physical characteristics brought change of seawater flow, sedimentary facies, and ecology of Yeongsan-river estuary. In the case of phytoplankton, primary producer in the marine ecology, size structure and biomass of basic source of food showed significant change by the artificial flood gate open and shut of estuary (Shin Dong, 2003) but from last 2004 to 2009, species furtherance of phytoplankton didn't show a significant difference in the change of marine environment(Cho, 2010). However, macrozoobenthos group of Yeongsan-river estuary showed about 20% decrease during last 10 years in the number of appearance species and average density showed about 40% decrease, and groups are changing due to appearance of species known as indicator species of contamination organism and density reduction of main dominant species(Lim and Seo, 2011). Such change can be significant factor on how long the low salinity water stays in the semiclosed ocean and the environment repeating inflow and block of fresh water. Also, in the aspect that salinity is preserved, behavior of many other water quality factors inflowing into ocean through behavior of low salinity water can be inferred. In the viewpoint, many researches on marine environment and ecology change of Yeongsan-river estuary were fulfilled but researches on the most basic low salinity water behavior influencing greatly the marine environment weren't accomplished much. Therefore, the study, by using 3 dimensional hydromechanics model, EFDC, predicted range of low salinity expansion by fresh water inflow before and after tidal gate extension in a flood season when fresh water inflow is the most and investigated low salinity water behavior as time passed.

II. Method

The EFDC (Environmental Fluid Dynamics Code) model was used to simulate the movement of seawater in the target waters and to pre-

dict the behavior of low salinity water. EFDC was developed by Virginia Institute of Marine Science (Hamrick, 1992) and is a multivariate, finite difference model that can simulate two- and three-dimensional movement of seawater and substances. It allows for easy vertical and horizontal two-dimensionalization and three-dimensionalization, and makes it possible to find solutions for equations regarding 3D vertical statics, free surface, and vortex-averaged baroclinity and barotropy in diverse types of density fields. Because of this the model can be applied both to seawater and freshwater systems, and thus is suitable for this study.

1. Introduction of model

Eddy viscosity and diffusion in the vertical direction is based on the method introduced by Galperin's *et al*. (1988), which is a modified version of Mellor and Yamada's (1982) Level 2.5 Turbulent Closure Scheme. The bottom friction against friction is described as the loss of quantity of motion in the boundary layer between the sedimentary and water layers, and is expressed by an equation for eddy boundary layer that uses a quadric function regarding the velocity measured at the ocean floor. Because the EFDC model is designed to handle 3D intertidal zones in the neritic region by using a mass-conserving scheme, it is particularly well-suited to be applied to Korean coasts, which have an expansive distribution of intertidal zones.

The model uses a -grid, which always has the same number of layers regardless of changes in vertical depth. On a staggered or C grid, it uses numerical solutions with a second order in terms of space. In terms of time, it uses the mode decomposition method that separates the internal and external modes of the three time levels of the second order. Also, in the external mode it uses the implicit method for calculation, which allows for a long calculation time as long as the stability condition for the explicit method of advection scheme, including nonlinear accelerations, is satisfied. In the case of the difference method of advection transport algorithm, there are different methods to choose from: the central difference method can be used for time and space, the forward difference method can be used for time, and upwind difference shemes can be used for space. For time, depending on the situation, the explicit method can be applied for horizontal diffusions and the implicit method for vertical diffusions.

1) Continuity equation

$$\partial_t(m_x m_y \zeta) + \partial_x(m_y H u) + \partial_y(m_x H v) + \partial_z(m_x m_y w) \quad (1)$$

2) Equation of motion

$$\begin{aligned}&\partial_t(m_x m_y H u) + \partial_x(m_y H u u) + \partial_y(m_y H v u) + \partial_z(m_x m_y w u)\\ &-(m_x m_y f + v\partial_x m_y - u\partial_y m_x)Hv = -m_y H\partial_x(g\zeta + p)\\ &-m_y(\partial_x h - z\partial_x H)\partial_z p + \partial_z(m_x m_y H^{-1} A_v \partial_z u) + Q_u\\ &\partial_t(m_x m_y H v) + \partial_x(m_y H u v) + \partial_y(m_y H v v) + \partial_z(m_x m_y w v)\\ &-(m_x m_y f + v\partial_x m_y - u\partial_y m_x)Hu = -m_x H\partial_y(g\zeta + p)\\ &-m_x(\partial_y h - z\partial_y H)\partial_z p + \partial_z(m_x m_y H^{-1} A_v \partial_z v) + Q_v\end{aligned} \quad (2)$$

3) Depth-intergrated continuity equation (for vertical boundaries)

$$\partial_t(m\zeta) + \partial_x(m_y H\int_0^1 u dz) + \partial_y(m_x H\int_0^1 u dz) = 0 \quad (3)$$

4) Static equation

$$\partial_z p = -gH(\rho - \rho_0)\rho_0^{-1} = -gHb \quad (4)$$

Here,

u, v: Horizontal velocity components of the x- and y-direction

h, ζ: Depth of water, elevation

H: Total depth of water ()

m_x , m_y : Square root of the diagonal component of a metric tensor that satisfies $ds^2 = m_x^2 d_x^2 + m_y^2 d_y^2$, an arbritrary distance on the curvilinear coordinates system

w: Vertical velocity component on a converted, nondimensional vertical coordinates system z
This has the following relationship with , the vertical velocity on actual coordinates
$w = w^* - z(\partial_t \zeta + um_x^{-1}\partial_x \zeta + \upsilon m_y^{-1}\partial_y \zeta) + (1-z)(um_x^{-1}\partial_x h + \upsilon m_y^{-1}\partial_y h)$

p : Displacement from pressure, depth of water z to the average water pressure ($\rho_0 gH(1-z)$), divided by ρ_0

f : Coriolis parameter

ρ : Density

ρ_0 : Standard density

g : Acceleration of gravity

b: Buoyancy

A_υ: Vertical turbulent viscosity coefficient

Q_u , Q_υ: Momentum source-sink term

5) Vertical turbulent viscosity and turbulent diffusion coefficients

This is calculated by using the Second Moment Turbulence Closure Model (Mellor and Yamada, 1982; Galperin *et al*., 1988), and has the following relationship with the turbulence intensity(q), turbulence length scale(l), and Richardson number (R_q):

$$A_\upsilon = \phi_\upsilon ql = 0.4(1+36R_q)^{-1}(1+6R_q)^{-1}(1+8R_q)ql \quad (5)$$

$$A_b = \phi_b ql = 0.5(1+36R_q)^{-1}ql \quad (6)$$

$$R_q = \frac{gH\partial_z b}{q^2}\frac{I^2}{H^2} \quad (7)$$

ϕ_υ, ϕ_b represent the stability function. Also, based on the transport equation, the turbulence intensity and turbulence length scale are defined as follows:

$$\begin{aligned}&\partial_t(m_x m_y Hq^2) + \partial_x(m_y Huq^2) + \partial_y(m_x H\upsilon q^2)\\ &+ \partial_z(m_x m_y wq^2) = \partial_z(m_x m_y H^{-1}A_q \partial_z q^2) + Q_q\\ &+ 2m_x m_y H^{-1}A_\upsilon((\partial_z u)^2 + (\partial_z \upsilon)^2) + 2m_x m_y gA_b \partial_z b\\ &- 2m_x m_y H(B_1 l)^{-1}q^2\end{aligned} \quad (8)$$

$$\begin{aligned}&\partial_t(m_x m_y Hq^2 l) + \partial_x(m_y Huq^2 l) + \partial_y(m_x H\upsilon q^2 l)\\ &+ \partial_z(m_x m_y wq^2 l) = \partial_z(m_x m_y H^{-1}A_q \partial_z q^2 l) + Q_1\\ &+ m_x m_y H^{-1}E_1 lA_\upsilon((\partial_z u)^2 + (\partial_z \upsilon)^2 + (\partial_z \upsilon)^2)\\ &+ m_x m_y gE_1E_3 lA_b \partial_z b - m_x m_y HB_1^{-1}q^3(1+E_2(kL)^{-2}l^2)\end{aligned} \quad (9)$$

$$L^{-1} = H^{-1}(z^{-1} + (1-z)^{-1}) \quad (10)$$

Here, B_1, E_1, E_2, E_3: Empirical constant

Q_q , Q_1: Additional source-sink term

A_q : Vertical diffusion coefficient

A_υ: Vertical turbulent viscosity coefficient

2. Establishment of model

A 240-square-kilometer sea area that included the intertidal zone was set as the basic target area of the model. The calculation grid used by the model was Seagrid, which is based on the Curvilinear-orthogonal grid system. Horizontally, a Curvilinear-orthogonal grid with a mean deviation of 1.710 from the orthogonal point was used. The grid was made up of a total of 23,272 active cells, with 292 in the x-direction and 232 in the y-direction. Also, a variable grid system was selected, which made it possible to maintain a precise grid distance of at least 23.5m-62.2m from the area near the tidal gate. Vertically there were three layers, taking into account factors such as the calculation time and stability. When entering the depth of water, digital charts no. 301, 321, and 342 (source: Korea Hydrographic and Oceanographic Administration) were used. The calculation was carried out every 4 seconds for 17 days, and after verification it was carried out for 45 days in order to figure out the behavior of low salinity water. The target sea area is the Yellow Sea that includes the Mokpo Port, Hwawon Peninsula, and Yeongam Peninsula, where tidal currents are dominant. Therefore, for the tides along the open boundary, the harmonic constant from data published by the Korea Ocean Research and Development Institute was used: the amplitude and phase of M2, S2, K1, and O1 harmonic constituents were calculated for each of the 59 cells that make up the western boundary, and these values were then entered. For initial condition it was assumed that there

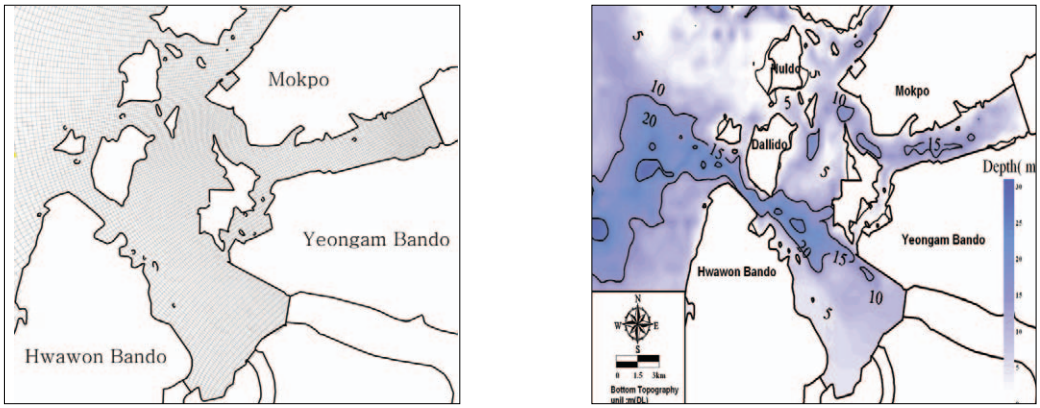

Grid map Bathymetric map

Fig. 1. Grid and bathymetric map of research sea area

Table 1. Average volume of freshwater inflow (1997~2009)

Category		Duration (days)	Average daily discharge time (min.)		Discharge volume per unit time (m^3/s)		Discharge volume per cell (m^3/s)	
			pre-expansion	post-expansion	pre-expansion	post-expansion	pre-expansion	post-expansion
Flood season	Yeongsan Lake	122	88.08	29.36	2,243.35	6,730.05	1,121.67(2)	1,121.67(2)
	Yeongam Lake		41.64	13.99	490.98	1472.94	163.66(3)	163.66(3)
	Geumho Lake		44.97	44.97	318.35	318.35	318.35(1)	318.35(1)

Note: Numbers inside parentheses represent the number of cells.

Table 2. Input data for salinity and water temperature

Category		Flood season		Note
		Water Temp.(℃)	Salinity (psu)	
Initial values		25.49	28.51	National Fisheries Research and Development Institute (1992-2008; average of 6 locations from Mokpo coastal areas and 1 location from Muan coastal areas)
Boun-daries	Surface layer	24.87	31.05	National Fisheries Research and Development Institute
	Bottom layer	23.59	31.88	(1992-2008; average of 2 locations from Sinan)
Yeongsan Lake		25.95	0	Ministry of Environment (1992-2008)
Yeongam Lake		22.42	0	
Geumho Lake		24.33	0	

was no movement of seawater, and Cold start was used. Also, in order to take into account the Coriolis force caused by the rotation of the Earth, 34°45′ north latitude (the central part of the calculated area) was entered.

3. Initial condition

The experiment was carried out before and after the expansion of the tidal gate during the flood season and normal season. The volume of freshwater inflow was entered as shown in Table 1, based on 13 years' worth of operation data of the tidal gate. After the tidal gate had been expanded, the gate was opened for shorter periods of time and the number of cells were increased. The period of discharge was 30 days, beginning from the start of the calculations. Then for the next 16 days, the inflow of freshwater

was cut off to observe the behavior of low salinity water as time passed by. Freshwater was discharged at low tide for the duration of the average daily discharge time. The temperature and salinity of freshwater from the lake was found through research and entered as shown in Table 2.

III. Results and discussion

1. Verification of hydrodynamic model

1) Tide

To verify how well the results from the hydrodynamic model simulated the current state, the results acquired from observations at Mokpo Tide Station were compared with the tidal time series results from the model's cells that represented the same location. This is shown in Table 3. In order to quantitatively estimate the accuracy of the model's results, the absolute relative error (ARE) and error were calculated for both the calculated and the observed results. As can be seen in Table 4, in the study the results calculated by the model was somewhat higher than the observed values for four major harmonic constituents. However, the ARE for amplitude and phase was below 15%, which shows that the tides of the target sea area were well simulated.

2) Tidal Current

To check how well the hydrodynamic model had simulated the present state, the tidal current values of the model cells that corresponded with the location of the observed values were verified using the time series verification of the east-west and north-south velocity components. This is shown in Table 5. As can be seen in Table 6, ARE was calculated for each average velocity of

Table 3. Location used to verify the tide levels

Observation point	Longitude	Latitude	Observation period
Mokpo Tide Station	126°22'39"E	34° 46'36"N	2009.01.01-2009.12.31

Note: Observation point (Ellipsoid: WGS84, Coordinate system: Geographic)

Table 4. Comparison of the observed and calculated values for tide levels

Category	M_2	ARE	ERROR	M_2	ARE	ERROR
	Amp(cm)	(%)	Amp(cm)	Phase(°)	(%)	Phase(°)
Observed	138.7	2.2	-3.0	29.6	13.2	-0.4
Model	141.7			33.5		
Category	S_2	ARE	ERROR	S_2	ARE	ERROR
	Amp(cm)	(%)	Amp(cm)	Phase(°)	(%)	Phase(°)
Observed	83.6	1.4	-0.6	79.7	3.7	3.0
Model	110.9			76.8		
Category	K_1	ARE	ERROR	K_1	ARE	ERROR
	Amp(cm)	(%)	Amp(cm)	Phase(°)	(%)	Phase(°)
Observed	45.8	1.5	0.4	248.7	4.8	12.0
Model	38.9			236.8		
Category	O_1	ARE	ERROR	O_1	ARE	ERROR
	Amp(cm)	(%)	Amp(cm)	Phase(°)	(%)	Phase(°)
Observed	26.6	14.8	3.5	213.8	7.3	-15.6
Model	30.8			229.4		

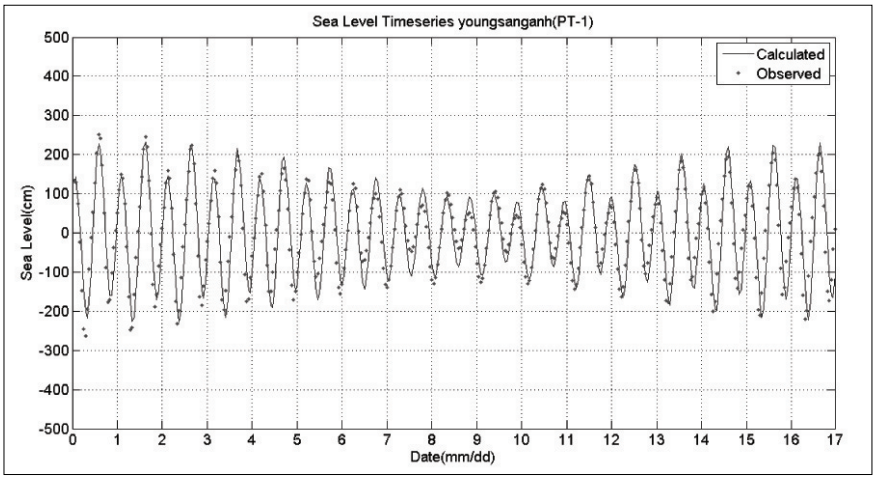

Fig. 2. Tidal calibration curve

Table 5. Location used to verify the tidal currents

Observation point	Longitude	Latitude	Observation period	Observation layer
*PC-1	E126°21'37.1"	N34°48'44.0"	2010.1.9.~2010.1.24.(15 days)	Surface layer
*PC-2	E126°18'11.9"	N34°45'35.4"		
*PC-3	E126°14'26.6"	N34°48'02.7"		
SC-1	E126°26'31.5"	N34°46'58.1"	2011.11.25.~2011.11.26.(25 hours)	Surface & Bottom layer

Note: Observation point (Ellipsoid: WGS84, Coordinate system: Geographic)
Source: *Environmental Impact Statement for Yeongsan River Estuary Bank Enhancement Project, Korea Rural Community Corporation, June 2010.

Table 6. Comparison of the calculated and observed values for average velocity of tidal currents

Category		Average velocity (cm/sec)	ARE(%)
PC-1	Observed	49.3	6.9
	Model	52.7	
PC-2	Observed	42.5	4.7
	Model	44.5	
PC-3	Observed	46.3	8.6
	Model	42.3	
SC-1(Surface)	Observed	3.7	5.4
	Model	3.5	
SC-1(Bottom)	Observed	3.0	3.3
	Model	3.1	

currents, and a time series plot that showed the east-west and north-south velocity components was drawn up for comparison. The results showed that although there were some minor differences in the velocity of currents (maximum ARE = 8.6%), the patterns of tidal currents of the east-west and north-south velocity components were quite similar, as can be seen in fig. 3.

2. Comparison of salinity distribution

The results of the salinity distribution experiment were compared with observed values for verification. The results from the observations made prior to May 28th, 2010 (i.e. before the expansion of the tidal gate) were compared with the results from the 16th day after the last discharge of freshwater, as predicted by the model. Similarly, the results from the observations made after the tidal gate was opened were compared with the results for the first hour after the last discharge of freshwater, also predicted by the model. As can be seen in figs. 4 and 5, this verifi-

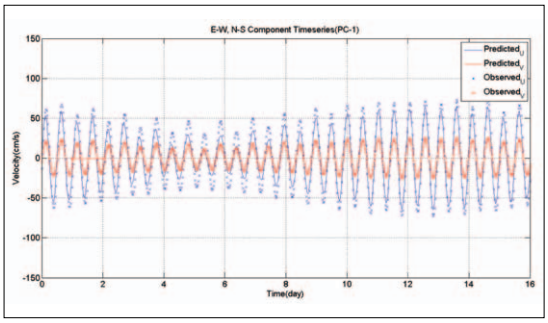

PC-1

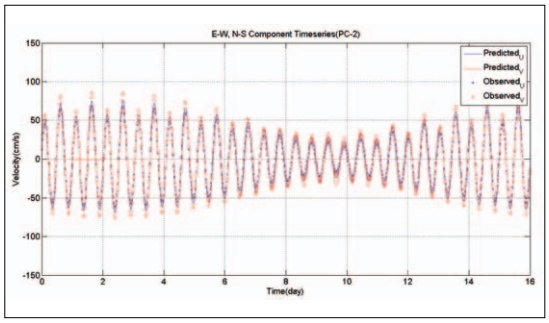

PC-2

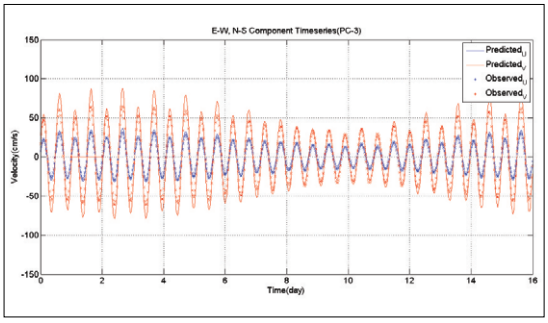

PC-3

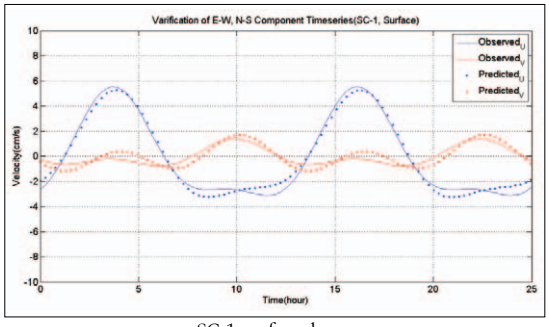

SC-1 surface layer

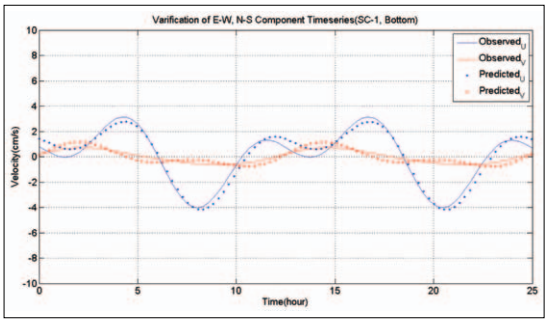

SC-1 bottom layer

Fig. 3. Tidal time series verification

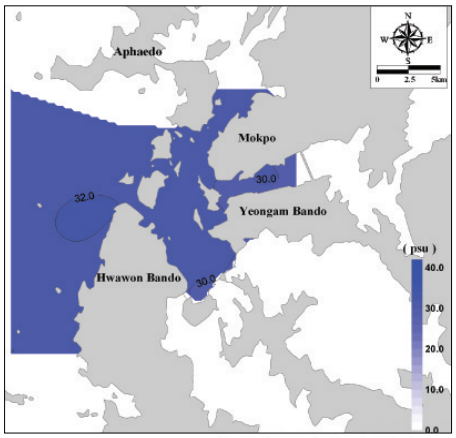

Surface layer (observed; before the tidal gate was opened)

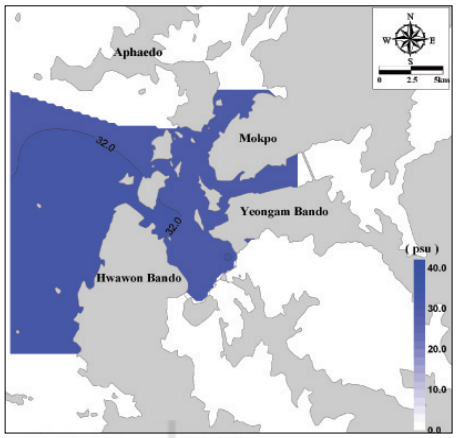

Bottom layer (observed; before the tidal gate was opened)

Fig. 4. Salinity distribution in a semi-normal state (without freshwater inflow)

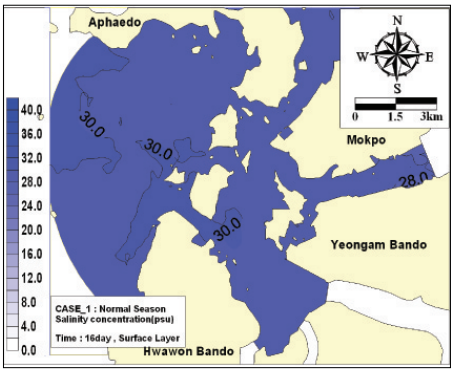

Surface layer (calculated by the model; after 16 days had passed)

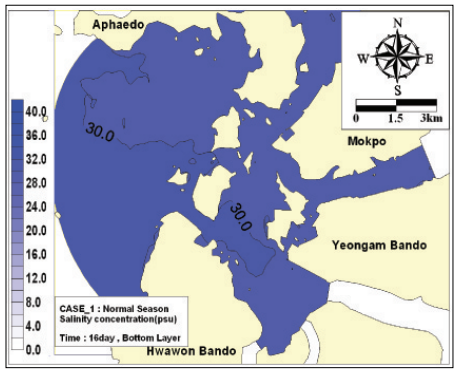

Bottom layer (calculated by the model; after 16 days had passed)

Fig. 4. Continued

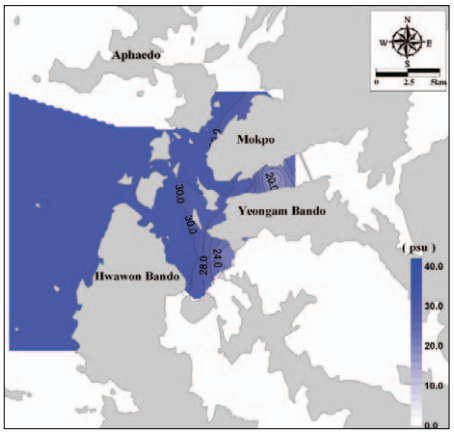

Surface layer (observed; after the tidal gate was opened)

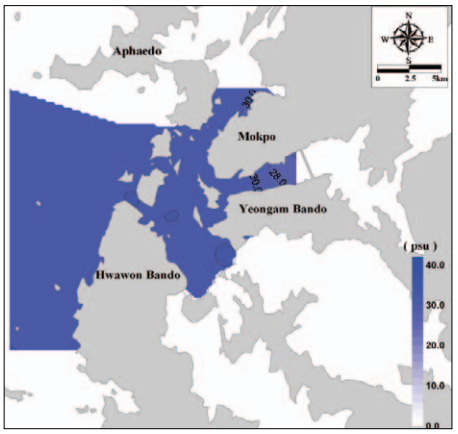

Bottom layer (observed; after the tidal gate was opened)

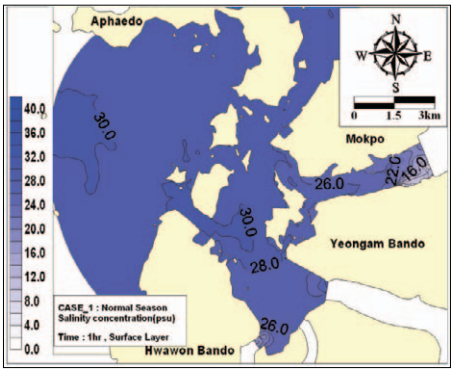

Surface layer (calculated by the model; after 1 hour had passed)

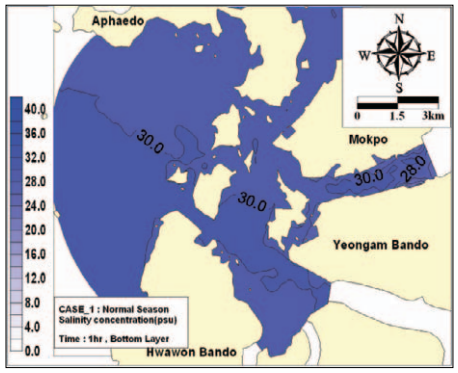

Bottom layer (calculated by the model; after 1 hour had passed)

Fig. 5. Salinity distribution after the tidal gate had been opened (with freshwater inflow)

cation showed that the calculated salinity distribution in the surface layer and bottom layer was relatively consistent with that observed before and after the opening of the tidal gate.

3. Low salinity water behavior before and after tidal gate extension

Regarding before and after tidal gate extension in the flood time, the extension results until 16days(45days after model fulfillment) in the

state of not accomplishing discharge from the last discharge time(0hr) after 30days from calculation starting time showed as Fig. 6~9 as time passed. In the results, low salinity water was distributed farthest toward ocean from tidal gate 6 hours later after fresh water inflow stopped, which is considered because low salinity water moved along ebb in the surface layer by density contrast

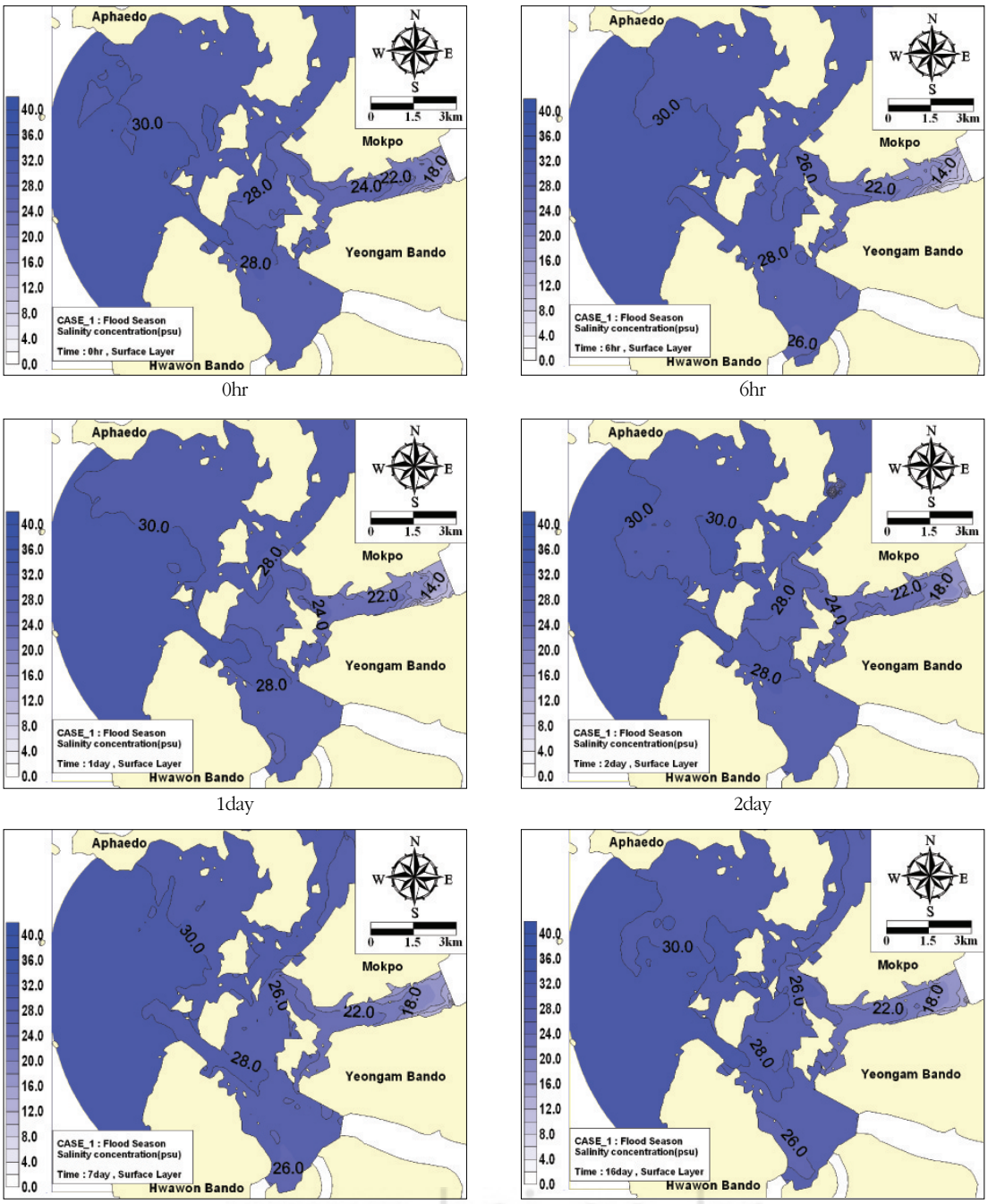

Fig. 6. Results from the salinity diffusion experiment according to time, before the expansion of the tidal gate

before refresh water is mixed by tidal current and warm current.

In the results comparing before and after tidal gate extension, low salinity water was distributed more farther from the tidal gate to ocean after the tidal gate extension than before, which is judged because discharge velocity was fortified by increase of discharge volume per hour after

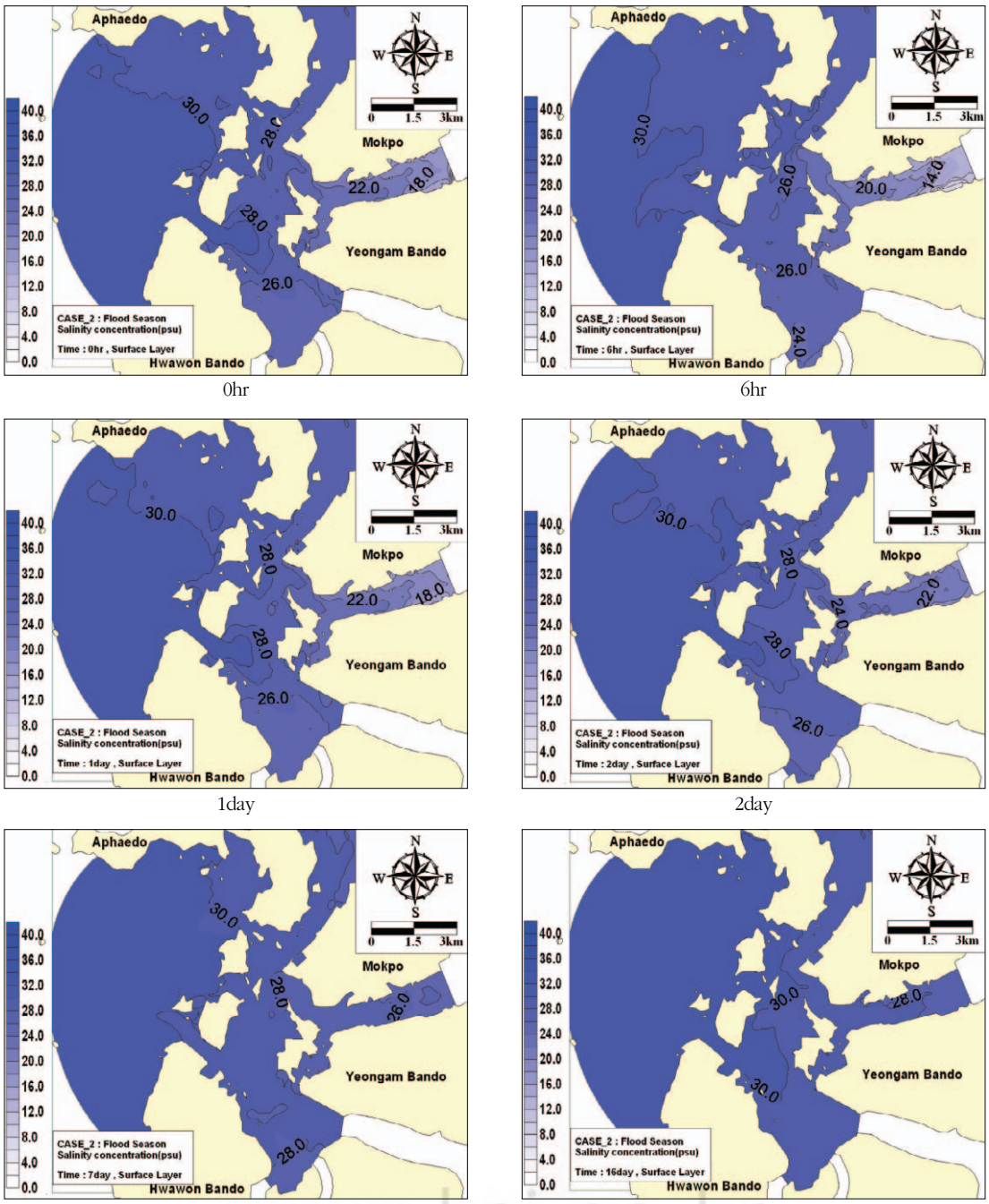

Fig. 7. Results from the salinity diffusion experiment according to time, after the expansion of the tidal gate

the tidal gate extension.

On the other hand, about 7 days from the stop of fresh water inflow before the tidal gate extension and after about 2 days passed after extension, salinity distribution pattern was close to the seminormality state before discharge, which implicates that in the state of no inflow of additional fresh water after fresh water inflow to coastal area by the tidal gate extension, salinity distribution of coastal area can reach quasistationary state by offshore water and inland sea water are mixed at least over 2~7 days later. Difference of low salinity water behavior pattern before and after the tidal gate extension is judged because discharge volume by hour increases by the tidal gate extension and discharge continuance time was reduced. In the end, since sea water mixture was intensified due to the increase of discharge volume by hour after the tidal gate extension, sea water mixture was activated than before the tidal gate extension and on the contrary discharge continuance time was reduced, and so it is judged the time of salinity distribution in the coastal area reaching quasistationary state was reduced.

IV. Conclusion

In order to figure out the behavior of low salinity water caused by the freshwater inflow in the Yeongsan River Estuary, this study predicted the salinity distribution using the EFDC model and reviewed the results. Experiment was fulfill by divided to before and after tidal gate extension and investigated low salinity water expansion pattern until reaching to the quasistationary state after 0hour, 2 hours, 1 day, 2 days, 7 days, and 16 days passed up to 16days(45days after fulfilling model) in the state of no discharge from the last discharge time after 30days of model fulfillment.

The results showed that the calculated salinity distribution for the surface and bottom layers were relatively consistent with the results from observations made before and after the expansion of the gate, and that the low salinity water in the surface layer spread farthest from the gate 6 hours after the discharge of freshwater, both before and after the gate expansion. Meanwhile, in the case of before tidal gate extension, salinity distribution showed similar pattern to the quasistationary state after about 7 days passed from the stop of fresh water inflow and in the case of after tidal gate extension showed similar distribution to the quasistationary state after about 2 days passed. As it was shown at Fig. 6~9, the time of coastal area after refresh water inflow reaching quasistationary state was shorter after tidal gate extension than before, which is judged because increase of discharge volume fortified turbulent mixing and low salinity water extended farther from coastal area was easily mixed comparing with offshore water. Therefore, in the case of that a certain amount of fresh water inflows to the coastal area, it is considered that extension of low salinity water has big discharge volume per hour and the shorter is the discharge continuance time, the shorter is the time of coastal area reaching quasistationary state.

Bibliography

Kang J.H., 1996, Environmental changes caused by the construction of an estuary dam and tide embankment in the Mokpo sea area, Journal of the Korean Society of Civil Engineers, 16,

611-619. (in Korean)

Kang J.H. and Im B.S., 1998, Changes in pollution diffusion patterns in the Mokpo sea area caused by the construction of tide embankment, Journal of the Korean Society of Civil Engineers, 18, 613-622. (in Korean)

Park R.H., Cho Y.G., Cho C., Seon Y.J. and Park G.Y., 2001, Seawater characteristics and circulation in the Yeongsan River Estuary in summer of 2000, Journal of the Korean Society of Oceanography, 6, 218-224. (in Korean)

Shin Young Sik, Seo Ho Young, Hyun Bong Gil, 2005, Effect of salinity change of sea water layer on size structure of primary producer and upper consumer, Journal of the Korean Society of Oceanography, the 10th, No. 2, 113-123.

Lee S.W., 1994, Changes in tidal level in Mokpo Port caused by the construction of the Yeongsan River Estuary Dam, Journal of the Korea Port and Harbor Association, 18, 27-37. (in Korean)

Lee Jung Woo, Shin Seong Ho, 1991, Numerical experiment on tide change by large-scale reclaimed land development, the 5th, No. 2, 65-75.

Lim Hyun Sik, Seo Chong Hyun, 2011, Change before and after 10 years of zoobenthos group structure of the Yeongsan River Estuary, Journal of the Korean Society of Oceanography, the 16th, No. 4, 254-267.

Cho Eun Seop, 2010, Water quality of coastal area of Mokpo Port and characteristics of phytoplankton change, Collection of dissertations of conference of Marine Environment Safety Society, 251-252.

Choi B.H., 1984, Changes in tidal level caused by the construction of tide embankment in the Yeongsan River Estuary, Journal of the Korean Society of Civil Engineers, 4, 113-124. (in Korean)

George L. Mellor, Tetsuji Yamada, 1982, Development of a Turbulence Closure Model for Geophysical Fluid Problems, Reviews of geophysics and space physics, 20, 851-875.

B. Galperin, A. Rosati, L.H. Kantha and G.L. Mellor, Modeling Rotating Stratified Turbulent Flows with Application to Oceanic Mixed Layers.

Fischer HB, List EJ, Koh RCY, Imberger J, Brooks NH, 1979, Mixing in inland and coastal waters. Academic, New York

Hamrick JM, 1996, Users manual for the environmental fluid dynamic computer code. The college of William and Mary, Virginia Institute of Marine Science, Special Report 328, 224 pp

최종원고채택 12. 07. 09